

# Assessment of the Inflammatory Effects of Gut Microbiota from Human Twins Discordant for Ulcerative Colitis on Germ-free Mice

Lina A Knudsen, MSc, PhD,<sup>1,2</sup> Line SF Zachariassen, DVM, PhD,<sup>3</sup> Mikael L Strube, MSc, PhD,<sup>4</sup>  
Jesper F Havelund, MSc, PhD,<sup>5</sup> Bartosz Pilecki, MSc, PhD,<sup>7</sup> Anders B Nexoe, MSc,<sup>7</sup> Frederik T Møller, MD, PhD,<sup>8</sup>  
Signe B Sørensen, MSc, PhD,<sup>1,7</sup> Niels Marcussen, MD, DMSci,<sup>9</sup> Nils J Færgeman, MSc, PhD,<sup>5</sup>  
Andre Franke, Dipl Biol, Dr.rer.nat,<sup>6</sup> Corinna Bang, Dipl Biol, PhD,<sup>6</sup> Uffe Holmskov, MD, PhD, DMSci,<sup>7</sup>  
Axel K Hansen, DVM, DVSci,<sup>3,\*</sup> and Vibeke Andersen, MD, DMSci,<sup>1,2,7,†</sup>

Disturbances in gut microbiota are prevalent in inflammatory bowel disease (IBD), which includes ulcerative colitis (UC). However, whether these disturbances contribute to development of the disease or are a result of the disease is unclear. In pairs of human twins discordant for IBD, the healthy twin has a higher risk of developing IBD and a gut microbiota that is more similar to that of IBD patients as compared with healthy individuals. Furthermore, appropriate medical treatment may mitigate these disturbances. To study the correlation between microbiota and IBD, we transferred stool samples from a discordant human twin pair: one twin being healthy and the other receiving treatment for UC. The stool samples were transferred from the disease-discordant twins to germ-free pregnant dams. Colitis was induced in the offspring using dextran sodium sulfate. As compared with offspring born to mice dams inoculated with stool from the healthy cotwin, offspring born to dams inoculated with stool from the UC-afflicted twin had a lower disease activity index, less gut inflammation, and a microbiota characterized by higher  $\alpha$  diversity and a more antiinflammatory profile that included the presence and higher abundance of antiinflammatory species such as *Akkermansia* spp., *Bacteroides* spp., and *Parabacteroides* spp. These findings suggest that the microbiota from the healthy twin may have had greater inflammatory properties than did that of the twin undergoing UC treatment.

**Abbreviations and Acronyms:** DAI, daily disease activity index; DSS, dextran sodium sulfate; IBD, inflammatory bowel disease; UC, ulcerative colitis

DOI: 10.30802/AALAS-CM-23-000065

## Introduction

Ulcerative colitis (UC), characterized by inflammation and ulcers in the colon and rectum,<sup>17,33</sup> is part of the human chronic disease spectrum termed inflammatory bowel disease (IBD). While some human patients respond to standard treatment, others may require surgical interventions despite advanced therapies. The precise etiology of IBD remains largely elusive; however, a consensus is emerging that it arises from a combination of genetic, immunologic, environmental, and gut microbiota factors.<sup>2,35</sup> Given the absence of a cure or predictive tools for disease trajectory, coupled with the global increase in its prevalence,<sup>22</sup> a pressing need exists for a deeper comprehension

of the disease's nature and the determinants of its severity. Consequently, numerous studies have examined the gut microbiota of human IBD patients.<sup>51</sup> Evidence indicates that an imbalance favoring proinflammatory over antiinflammatory bacteria contributes to the disease origin.<sup>64</sup> Specifically, IBD-prone individuals show a decline in diversity and reduced abundance of Firmicutes.<sup>65,75,76</sup> Diminished Bacteroidetes and elevated Proteobacteria levels are also associated with IBD.<sup>51</sup> Nonetheless, conflicting findings have also surfaced,<sup>1</sup> particularly with regard to the influence of IBD treatments in steering gut microbiota toward a more beneficial profile.<sup>30,37,42,80</sup> Interactions of gut microbiota, diet, and various treatments have been reported.<sup>3,44</sup> Given the apparent impact of host genetics on gut microbiota composition on IBD,<sup>36</sup> an important determination is whether differences in specific taxa in patients and controls are due to the disease, dietary choices, medication regimens, or genetics. Consequently, identifying gut microbiota components that trigger or contribute to disease onset is a complex undertaking.

In recent years, one research approach has been to mimic the phenotype induced by a particular human gut microbiota composition by transferring human gut material into germ-free mice.<sup>23</sup> This colonization results in a stable microbiota in the transplanted animals, even across different housing conditions and generations.<sup>40</sup> This methodology has successfully replicated the obese phenotype of human patients in mice,<sup>60</sup> while multiple

Submitted: 10 Oct 2023. Revision requested: 12 Dec 2023. Accepted: 15 Feb 2024.

<sup>1</sup>Medical Department, Molecular Diagnostic and Clinical Research, University Hospital of Southern Denmark, Aabenraa, Denmark; <sup>2</sup>IRS-Center Sønderjylland, University of Southern Denmark, Odense, Denmark; <sup>3</sup>Department of Veterinary and Animal Sciences, Faculty of Health and Medical Sciences, University of Copenhagen, Frederiksberg C, Denmark; <sup>4</sup>DTU Bioengineering, Technical University of Denmark, Lyngby, Denmark; <sup>5</sup>VILLUM Center for Bioanalytical Sciences, Department of Biochemistry and Molecular Biology, University of Southern Denmark, Odense M, Denmark; <sup>6</sup>Institute of Clinical Molecular Biology, Christian-Albrechts-University of Kiel, Kiel, Germany; <sup>7</sup>Department of Molecular Medicine, University of Southern Denmark, Odense, Denmark; <sup>8</sup>Department of Infectious Disease Epidemiology and Prevention, Statens Serum Institut, Copenhagen, Denmark; and <sup>9</sup>Department of Clinical Pathology, Odense University Hospital, Odense, Denmark

\*Corresponding author. Email: akh@sund.ku.dk

†These authors contributed equally to this study

microbiota transplantations have established an inducible humanized microbiota mouse model for IBD, employing stool samples from IBD patients exhibiting varying degrees of disease activity.<sup>12</sup> Experimental mouse models that exhibit key human IBD traits<sup>41</sup> can be chemically induced using methods such as oral administration of dextran sodium sulfate (DSS) or rectal application of haptens like oxazolone.<sup>8</sup>

In human cotwins discordant for IBD, the healthy twin has a higher risk of developing IBD as compared with the general population.<sup>11,24</sup> Recent findings suggest that the healthy cotwin gut microbiota is more similar to that of their affected twin or IBD patients in general, as compared with healthy individuals.<sup>11</sup> It is conceivable that over a lifetime, the twin diagnosed with IBD will have undergone numerous treatments and lifestyle adjustments, including dietary modifications. Therefore, we hypothesized that in some human twin pairs, the twin with IBD may have developed a gut microbiota with less inflammatory potential and better protection against IBD than that of the healthy twin. Thus, we conducted a study to compare induction of IBD in offspring of pregnant mice inoculated with fecal samples from one of 2 discordant twins: one healthy and the other afflicted with UC.

## Materials and Methods

**Ethics.** All animal experiments were carried out in accordance with the Danish Act on Animal Experimentation (LBK No 1107 of July 1, 2022).<sup>54</sup> The study was approved by the Animal Experimentation Inspectorate, Ministry of Food, Fisheries and Agriculture, Denmark (license number 2012-15-2934-00256) and was planned in accordance with the PREPARE guidelines<sup>66</sup> and reported in accordance with ARRIVE guidelines.<sup>56</sup> Humane endpoints were defined as weight loss greater than 20% of expected weight, reduced appetite, reduced activity, visible blood in feces, and/or rectal prolapse. The human twin sample used for this specific study was recruited and collected between July 1, 2013, and December 31, 2013, as approved by the Ethics Committee of the Region of Southern Denmark (S20120176) and the Danish Data Protection Agency (2008-58-035). Informed verbal consent and written consent were obtained from all subjects.

**Animals, donors, and procedures.** Eight to 12 germ-free Swiss Webster (Tac:SW) mice (4 to 6 females, 4 to 6 males) (Taconic Biosciences, Germantown, NY) were set up for pair breeding at 7 wk in our AAALAC-accredited isolator facility (Faculty of Health and Medical Sciences, University of Copenhagen, Frederiksberg, Denmark) in HEPA-ventilated isolators (PFI Systems, Milton Keynes, UK) (pressure 110 Pa, 23 °C). Mice were housed with a light:dark cycle of 12:12 h and received an irradiated Altromin 1314 diet (Brogarden) and sterilized water ad libitum. Germ-free status of the recipients was confirmed by the absence of bacteria in aerobic and anaerobic cultivation and 16S PCR.<sup>81</sup>

Human stool samples for inoculation of mice were obtained from a previously described Danish monozygotic IBD twin cohort.<sup>47</sup> A pair of human twins discordant for UC was selected as donors. The twins were female, were 51 y of age at sampling, and had BMIs of 28.72 (overweight) and 33.41 (obesity class I)<sup>16</sup> for the UC twin and healthy cotwin, respectively). Neither twin had been treated with antibiotics during the 3 mo before sampling. The UC donor had remittent UC and had been diagnosed 20 y earlier. At sampling, the UC twin was receiving the standard medical treatment of 5-aminosalicylic acid.<sup>47</sup> She reported not having active disease at the time of sampling, had a simple clinical colitis activity index score of 4 (inactive disease 0 to 4, active disease 5 to 19),<sup>77</sup> and had a fecal calprotectin level of 379 ng/L,<sup>14</sup> (a component of neutrophil cytosol

that provides a rough measure of inflammatory activity).<sup>55</sup> The healthy cotwin had a colitis score of one and a fecal calprotectin level of 22 ng/L. The pairwise Bray–Curtis dissimilarity percent for the twin pair was 66.5% and was calculated from 16S rDNA sequencing (V3-V4) data from the human stool samples (unpublished results).

The human stool samples were collected according to the Sample PREanalytical Code and Biospecimen Reporting for Improved Study Quality guidelines.<sup>9,49</sup> The twins collected their own stool specimens and stored the samples in their home freezer at –20 °C.<sup>47</sup> At collection from the participants' homes, samples were transferred immediately to a –80 °C freezer, which has been reported as optimal to ensure stool samples are stable in composition.<sup>79</sup>

Germ-free pregnant Swiss Webster mice were transferred in an aseptic manner from the breeding isolator to 2 inoculation isolators and were inoculated with stool from either the healthy twin (referred to in figures and tables as “Healthy” mice) or the UC twin (referred to in figures and tables as “UC” mice). The human stool samples (200 µL per sample, previously stored at –80 °C) were suspended approximately 1:5 in sterile PBS in a laminar flow hood. Two to 3 pregnant female germ-free mice were used for each inoculum, and they were inoculated by oral gavage with 200 µL human stool in PBS. Any excess sample was distributed evenly on the fur of the inoculated mice to increase the likelihood that the offspring would have a microbiota as similar as possible to the original sample. An additional aliquot of PBS-suspended stool sample was distributed on the fur of the offspring and mammae of the mother at 1 and 3 wk after birth. Previous studies report that colonization in this manner remains stable over generations.<sup>40</sup>

The pups were weaned at 3 wk of age and separated into same-sex experimental groups within each litter. The mice were then removed from the isolators and housed IVCs (Tecniplast, Buguggiate, Italy) at one to 4 mice per cage under standard laboratory conditions (a 12-h light:dark cycle and free access to demineralized water and food [nonirradiated Altromin 1314, Lage, Germany]) at the Biomedical Laboratory, University of Southern Denmark, Odense, Denmark. The 2 groups were housed in separate IVC systems and gloves were changed between handlings. The room was controlled at 55% relative humidity and 22 ± 3 °C, and animal health status was monitored according to FELASA guidelines.<sup>43</sup> Entry into the animal facility required donning protective clothing, disposable hats, and dedicated shoes in a change room. Gloves were mandatory when touching or handling animals.

**Dextran sodium sulfate experiment and sample collection.** The study design and timeline are illustrated in Figure 1. The offspring (8 to 9 wk old) (Healthy-inoc  $n = 24$  [12 males, 12 females] and UC-inoc  $n = 13$  [4 males, 9 females]) were given demineralized water containing 1.5% DSS (MP Biomedicals, Solon, OH) ad libitum for 7 d to induce colitis. On the eighth day, mice began to receive demineralized water without DSS. Mice were euthanized by CO<sub>2</sub> asphyxiation on day 10 after initiation of DSS but were euthanized prematurely if one or more of the aforementioned humane endpoints were reached. Four mice were euthanized prematurely when they reached the aforementioned humane endpoints (2 mice on day 7 and 2 on day 9).

Fresh stool samples were collected from mice at baseline (before DSS) and on days 7 and 10. At euthanasia, colon length was measured, and cecum content was collected. The murine colon was dissected and flushed with ice-cold PBS. Then, 1.5 cm of colonic tissue was fixed for 24 h in 4% formaldehyde, divided

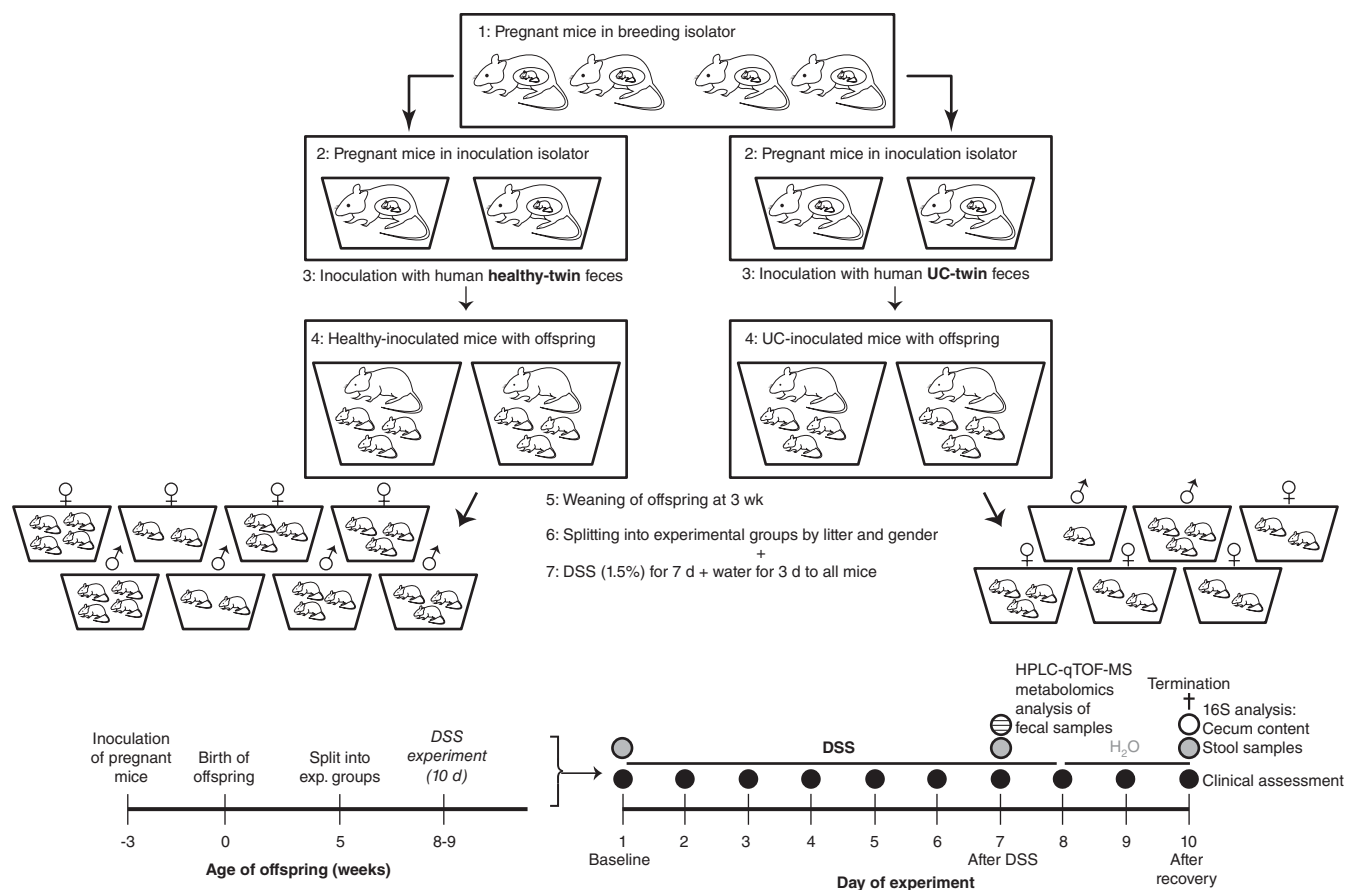


**Figure 1.** Experimental setup and timeline. After mating, pregnant germ-free mice were transferred from the breeding isolator into 2 different isolators for inoculation with stool from either the healthy or the ulcerative colitis (UC) twin. The offspring remained in the isolators with their mothers until weaning at approximately 3 wk of age. At approximately 5 wk of age, all offspring were removed from the isolators and separated into experimental groups based on litter and sex. When the mice had reached 8 to 9 wk of age, dextran sulfate sodium (DSS) exposure was initiated by giving all mice drinking water containing 1.5% (w/v) DSS ad libitum (baseline/day 1). On the morning on day 8, the DSS water was substituted with pure drinking water. Mice were euthanized on day 10.

into 3 transverse fragments of 5 mm, and transferred to PBS with 0.1% azide (all at 4 °C) for storage before being embedded in paraffin. All other samples were snap-frozen in liquid nitrogen and stored at –80 °C until analysis.

**Blinding.** When handling and assessing the mice, the daily care staff and the clinical assessor were blind to which human stool sample each cage of mice had received. An experienced pathologist who was blind to treatment group assessed and scored histologic findings. For the 16S and metabolomics analyses, the 2 groups were assigned the names ‘donor 0’ and ‘donor 1,’ such that the data analyst was blind to the sample origin.

**Clinical assessment.** Body weight, fecal score, and fecal blood score were assessed on individual fecal samples every day from baseline until euthanasia. Occult fecal blood was evaluated using the Hemocult Sensa FOB-test (Beckman Coulter). Factors were scored according to Table 1, and scores were added to give a daily disease activity index (DAI) score, as modified from a previous publication.<sup>29</sup> A similar DAI protocol is available at Bio-Protocol Exchange.<sup>32</sup>

**Histology.** Formalin-fixed colon samples were paraffin-embedded, cut in 4 μm sections, and stained with hematoxylin-eosin. Variables were assessed and scored for the degree of lamina propria inflammatory cell infiltration, muscularis mucosae thickening, goblet cell depletion, and the presence of crypt abscesses (Table 1), as previously described.<sup>10</sup> Scores for

each category were summed, resulting in possible total scores of between 0 (not inflamed) and 11 (inflamed).

**16S rDNA sequencing.** The fecal microbiota from baseline, day 7, and day 10 and cecum content was characterized by high-throughput sequencing. Samples were not available from all mice at all time points. Numbers of samples were as follows: baseline: UC-inoc, 13 and Healthy-inoc, 24; day 7: UC-inoc, 12 and Healthy-inoc, 22; day 10: UC-inoc, 13 and Healthy-inoc, 19; cecum content: UC-inoc, 13 and Healthy-inoc, 21. DNA was extracted using the QIAamp DNA stool mini kit automated on the QIA-cube (Qiagen, Aarhus, Denmark). Approximately 200 mg of the fecal sample was transferred to 0.70 mm Garnet Bead tubes filled with 1.1 mL ASL lysis buffer (containing Proteinase K; Qiagen). Bead beating was then performed using the SpeedMill PLUS (Analytik Jena, Jena, Germany) for 45 s at 50 Hz. Samples were then heated to 95 °C for 5 min. PCR inhibitors were removed by the combined action of InhibitEX (a unique adsorption resin; InhibitEX, Alpharetta, GA), and an optimized buffer. Variable regions V3/V4 of the 16S rRNA gene were amplified using the primer pair 341F-805R in a dual-barcoding approach. PCR products were verified through electrophoresis in agarose gel. PCR products were normalized using SeqPrep Normalization Plate Kit (Invitrogen, Waltham, MA), pooled equimolarly, quality controlled via agarose gel electrophoresis, and sequenced on the Illumina MiSeq (Illumina, San Diego, CA)

**Table 1.** Clinical and histologic scoring of inoculated DSS-induced mice

Disease activity index (DAI) scoring system					
Weight loss	Score	Feces	Score	Fecal blood	Score
<1%	0	Hard/firm	0	Negative	0
1% to 5%	1	Firm but sticky	1	Hidden	1
5% to 10%	2	Soft but still coherent	2	Visual	2
10% to 15%	3	Soft with loss of shape, mucus visible	3	Rectal bleeding	3
15% to 20%	4	liquid without any firm consistency	4		
Histologic damage score parameters					
Type of damage	Score				
	0	1	2	3	
Inflammation	Rare inflammatory cells in the lamina propria	Increased numbers of granulocytes in the lamina propria	Confluence of inflammatory cells extending into the submucosa	Transmural extension of inflammatory infiltrate and ulceration of the mucosa	
Crypt abscess	Absent	Present			
Goblet cell depletion	Absent	Present			
Degree of goblet cell depletion	Normal (no depletion)	Small decrease in number of goblet cells	Pronounced goblet cell depletion but goblet cells present in all areas	Severe goblet cell depletion; no goblet cells present in some areas	
Muscle thickening (base of crypt on the muscularis mucosa)	Absent	Slight	Moderate	Marked	

(2 × 300bp). Sequencing data were quality cleaned, merged, chimera checked, and classified with BION-meta (Metabion, Planegg, Germany) using the Ribosomal Database Project. Colonization efficiency was calculated by identifying the number of taxa on genus level in the sampled mice and determining the fraction compared with the taxa in the inoculum.<sup>40</sup>

**Fecal metabolite profiling.** Metabolite extraction was performed on stool samples from mice ( $n_{UC-inoc.} = 12, n_{Healthy-inoc.} = 20$ ; samples were not available from all mice) as previously described with minor alterations.<sup>39</sup> Briefly, the stool sample (40 mg) was dissolved in a 640 μL cold methanol:water (v/v 1:1) mixture containing 1 pmol/μL internal standard (C13-labeled amino acids). Samples were vortexed at maximum speed for 10 min using a flat-bed vortex, and the supernatant was centrifuged for 30 min at maximum speed (21,000 × g) at 4 °C, filtered through a 13-mm 0.2-μm filter, and dried in a SpeedVac (HetoVac VR-1; Heto Lab Equipment, Allerød, Denmark). The lyophilized samples were resuspended in 30 μL 1% aqueous formic acid and injected using an Agilent 1290 Infinity HPLC system coupled to a Q-TOF mass spectrometer (model 6530; Agilent Technologies, Santa Clara, CA) and analyzed as previously reported<sup>28</sup> in both positive and negative ion modes.

Databases containing retention time and metabolites of annotated compounds were constructed according to the formula and experimental fragmentation data of Metabolomics Standards Initiative level 3.<sup>62</sup> Chromatograms were extracted and quantified using Profinder v. B.08.00 (Agilent Technologies) with a mass tolerance of 50 ppm and retention time tolerance of 0.1 min. An untargeted approach was also applied using MzMine.<sup>57</sup> The LC-MS data files were converted to the mzData format using the Agilent MassHunter Qualitative Analysis program (v. B.07.00) before processing using MZmine (v. 2.23). Molecular formulae were generated using isotopic patterns and searched against the Human Metabolite Database v. 3.6 (hmdb.ca) for putative annotations (Metabolomics Standards Initiative level 4). The lists from the targeted and untargeted data extractions were

combined. Peak intensities were normalized to total signals in the sample. Normalized data were filtered for highly variable signals, log transformed, and autoscaled using MetaboAnalyst<sup>18</sup> to create a PCA plot.

**Statistical analyses.** Welch *t* test was used to compare the 2 groups, and a Mann-Whitney *U* test was used for data with a non-Gaussian distribution or ordinal data. The area under the curve was used to compare weight loss data. 16S sequencing data were normalized to 100,000 reads before analysis. Barplots were presented as individual samples with the dominating 11 genera. Diversity was calculated as the Shannon index and tested with an ANOVA with Tukey post hoc test. Multivariate analysis was conducted by nonmetric multidimensional scaling on the family level, and meta-data was regressed onto the ordination by the envfit-function, all using the vegan package.<sup>52</sup> The significance of 16S data for individual bacteria was analyzed using the Kruskal-Wallis test followed by the Conover-Iman test with Sidak correction for multiple comparisons.

**Data availability.** The datasets generated and analyzed during the current study are available in the Mendeley Data repository at <https://data.mendeley.com/datasets/dfg449h2wt/1> and the Sequence Read Archive, accession number PRJNA809154, respectively.

## Results

**Colon inflammation.** Offspring whose dams had been inoculated with stool from the healthy twin had significantly higher clinical scores from day 3 of DSS onward as compared with mice whose dams were inoculated with stool from the UC twin (Figure 2A–D). Of the original 37 mice, 4 were prematurely euthanized upon reaching human endpoints; all 4 (16.7% of their group) had received stool from the healthy twin. The histologic damage score of the colon sections was significantly lower in mice that received stool from the UC twin as compared with those whose dam had been inoculated with stool from the

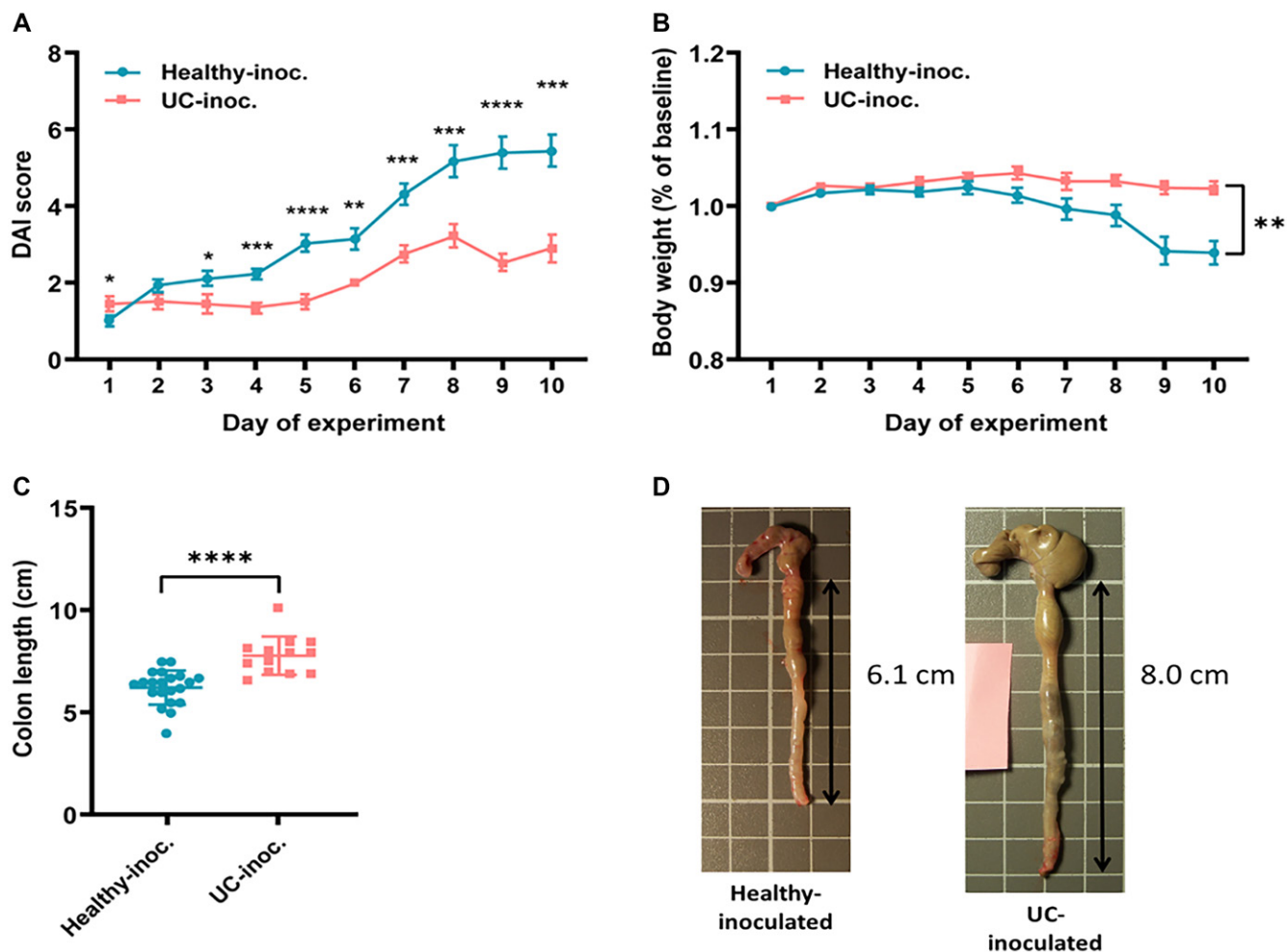


**Figure 2.** Clinical evaluation of Swiss-Webster mice (male/female; 8 to 9 wk at baseline) treated with dextran sodium sulfate (DSS) and inoculated with human stool. Mice inoculated with stool from the UC twin (UC) are denoted in red ( $n = 13$ ), and those inoculated with stool from the healthy cotwin (Healthy) are indicated in blue ( $n = 24$ ). These mice underwent a 7-d period of DSS in the drinking water (1.5% DSS), followed by 3 d of water without DSS. (A) The average total disease activity score  $\pm$  SEM for all mice, analyzed through individual day Mann-Whitney  $U$  tests. (B) The average body weight expressed as a percentage of the initial starting weight  $\pm$  SEM for all mice, evaluated using 2-way ANOVA. (C) The average colon length in centimeters  $\pm$  SEM for all mice, analyzed using an unpaired  $t$  test. (D) Visual representation of colon lengths from a mouse that received the Healthy inoculum and one that received the UC inoculum. Each square in the background of the images indicates  $1 \times 1$  cm. The 2 colons are representative of the typical presentation for each respective group of mice. \*,  $P < 0.05$ , \*\*,  $P < 0.01$ , \*\*\*,  $P < 0.001$ , \*\*\*\*,  $P < 0.0001$ . DAI, disease activity index.

healthy twin (Figure 3A). Microscopic analysis of the colon tissue displayed various characteristics of increased inflammation (Figure 3B).

**Microbiota.** Specific bacterial taxa exhibited varying patterns of presence. *Dialister* spp. and *Intestinibacter* spp. were predominant in the healthy twin's samples. Conversely, *Barnesiella* spp. and *Bacteroides* spp. were exclusive to the UC twin's samples (Figure 4). *Bacteroides* spp., including that both *B. vulgatus* and *B. fragilis*, known for their opposing roles in inflammation exacerbation and alleviation, respectively,<sup>61,63</sup> were consistently abundant at all time points in the UC twin. *Parabacteroides* spp. were predominantly present in mice inoculated with stool from the UC twin, with steady abundance from baseline to termination. The efficiency of colonization of offspring at baseline was approximately  $39 \pm 1\%$  and  $34 \pm 1\%$  (mean  $\pm$  SEM) for UC and healthy twin gut microbiota, respectively. The transfer of taxa from twin through the dam to their offspring was not consistent. *Faecalibacterium* spp., a taxon recognized for its antiinflammatory properties,<sup>67</sup> were prominent in both donors, yet did not establish in the mice. Conversely, unclassified Lachnospiraceae

and Porphyromonadaceae were effectively transferred from both twins to their respective groups of mice and were significant genera in the mouse microbiota, despite the low initial abundance in human donors. The most abundant genus found in the UC twin and mice inoculated with stool from the UC twin was *Bacteroides* (Table 2).

The antiinflammatory *Akkermansia* spp. were observed at relatively low levels in both twins. However, in mice, its abundance rose significantly throughout the experiment, particularly in mice that were inoculated with stool from the UC twin as compared with those inoculated with stool from the healthy twin (Table 2). Although *Prevotella* spp. were detected in both twins, *Paraprevotella* spp. were identified only in stool from the UC twin and subsequently were transferred only to the corresponding group of mice. A multivariate analysis demonstrated distinct clustering of the 2 groups of mice with regard to the bacterial composition of stool from the 2 donors (Figure 5A). The predominant taxa in the UC twin and the corresponding mice were Bacteroidaceae, Prevotellaceae, and Verrucomicrobiaceae. In contrast, the healthy twin and the corresponding mice

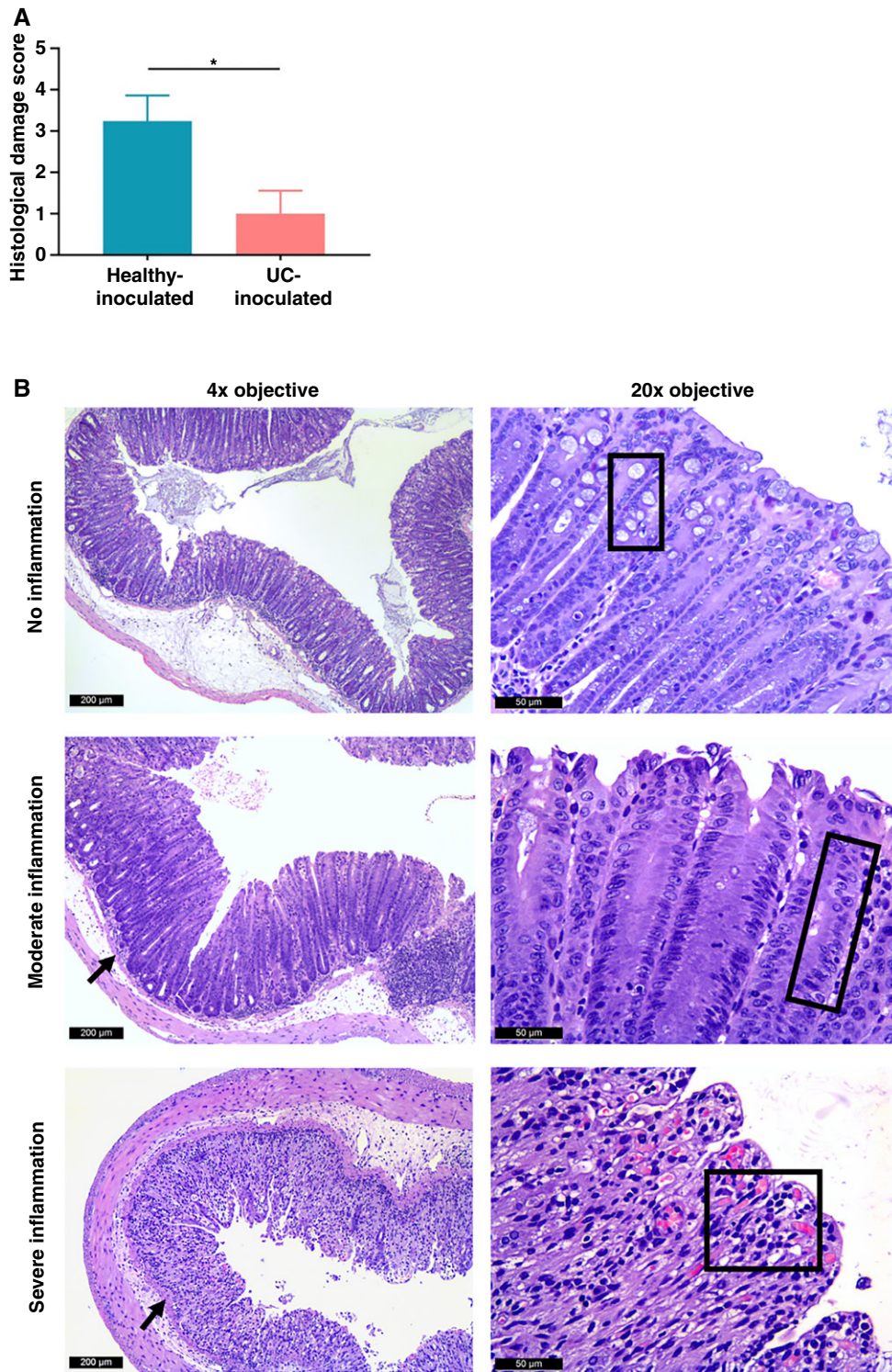


**Figure 3.** The histologic evaluation of Swiss-Webster mice (male/female; 8 to 9 wk old at baseline) that were inoculated with stool samples. (A) Histologic damage scores are shown as mean  $\pm$  SEM for colon sections from mice treated with dextran sodium sulfate (DSS) and inoculated with stool from the healthy twin (Healthy) in blue ( $n = 21$ ) and from the UC twin (UC) in red ( $n = 13$ ). The difference was assessed using the Mann-Whitney  $U$  test; \*,  $P < 0.05$ . (B) Hematoxylin and eosin were used to stain colon sections from DSS-treated mice, revealing varying degrees of inflammation. Images were captured using both 4 $\times$  and 20 $\times$  objectives. Representative sections are shown. The top sections show no pathologic damage; the 20 $\times$  objective image shows numerous goblet cells, as indicated by the black box. The middle sections show moderate pathologic changes, characterized by significant goblet cell depletion and a mild thickening of the muscularis mucosa (indicated by the black arrow). The 20 $\times$  objective image displays the absence of goblet cells, highlighted by the black box. The lower section shows severe pathologic alterations, including complete goblet cell depletion, substantial infiltration of inflammatory cells, and prominent thickening of the muscularis mucosa (indicated by the black arrow). In the 20 $\times$  objective image, the presence of abundant inflammatory cells is highlighted in the black box.

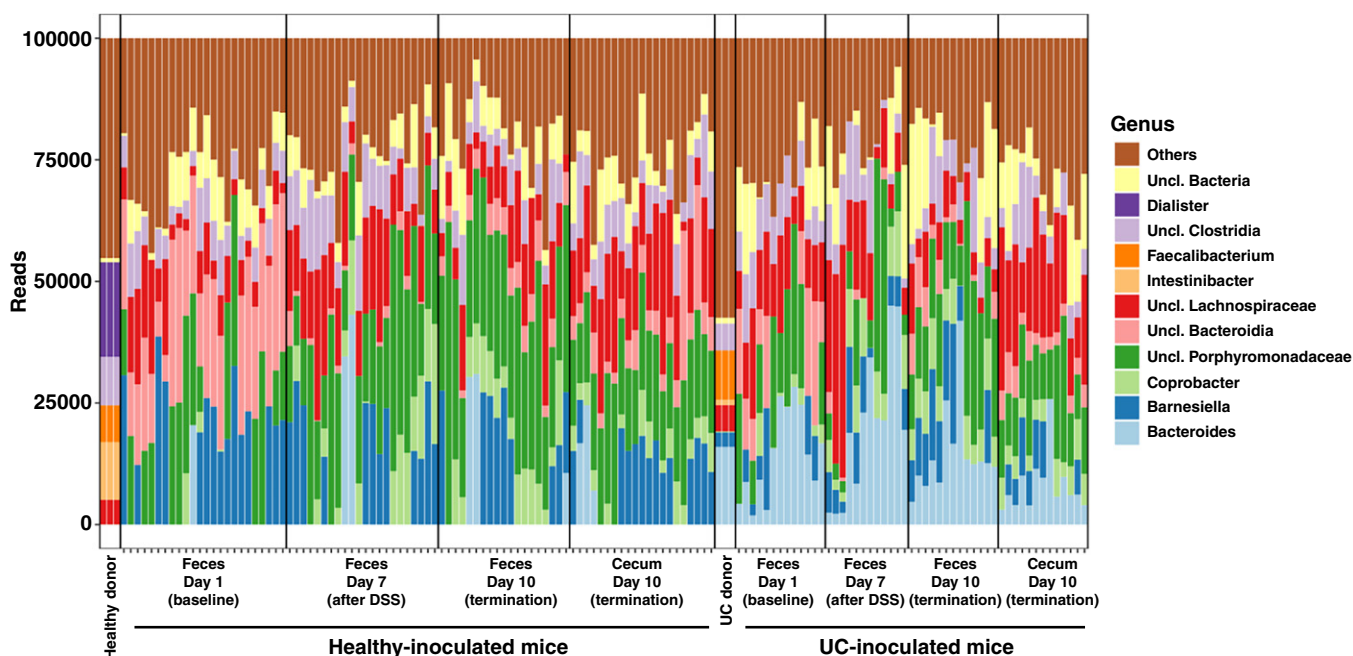


**Figure 4.** The taxonomic composition of the most abundant species of human donor stool samples from 2 discordant twins (one healthy and the other diagnosed with UC) and the mice respectively inoculated with stool from the healthy and UC donors. Data were obtained through 16S rDNA sequencing. Sampling occurred on day 1 (baseline), day 7 (after dextran sodium sulfate [DSS] challenge), and day 10 (euthanasia). Cecal content was also assessed at euthanasia. The taxonomic profiles of the 11 most abundant genera of bacteria are shown. Sample sizes are as follows: UC-inoculated: 13 at baseline, 12 on day 7, and 13 for feces and cecum on day 10; Healthy-inoculated: 24 at baseline, 22 on day 7, 19 fecal samples on day 10, and 21 cecal samples on day 10.

predominantly had unclassified Bacteroidia, Lactobacillaceae, Anaeroplasmataceae, and Eubacteriaceae (Figure 5A).

In the cecum, the distinctions in taxa between the 2 groups paralleled those observed in the stool samples collected on day 10. However, differences between groups were not significantly different when adjusted for multiple comparisons.

Alpha diversity, assessed at the family level (as depicted in Figure 5B), was significantly greater in both feces and cecum of mice that were inoculated with UC as compared with the other group. Although this difference was not significant at the genus level (Figure 5B), the genera present in these mice seemed to span a more extensive range of bacterial families than did the genera present in mice inoculated with stool from the healthy twin. After DSS challenge, diversity at the family level fell in both groups. Only mice inoculated with UC stool regained some of the lost diversity after the DSS was stopped; this recovery was also evident at the genus level. In contrast, the diversity at the genus level in mice inoculated with stool from the healthy twin was constant throughout the experiment. In essence, even though the immediate impact of the DSS challenge on the gut microbiota appeared to be more pronounced in the mice inoculated with UC stool, they also showed a more effective recovery as compared with the other group.

**Effects of DSS.** The DSS challenge appeared to have a uniform effect on the bacterial microbiota, as the qualitative and quantitative bacterial differences between the 2 groups were more obvious at baseline (Tables 2 and 3). Enterobacteriaceae, which are known to be associated with IBD<sup>74</sup> and are represented in this study mainly by *Escherichia* spp., were present only in mice inoculated with UC stool, but their abundance fell markedly after DSS administration. Although less abundant, Rikenellaceae, *Vallitalea* spp., and Clostridiaceae also fell in the UC mice after DSS administration, moving closer to

levels found in mice inoculated with healthy stool. Conversely, *Paraprevotella* spp. (which was found only in mice inoculated with UC stool) had a low abundance at baseline but increased significantly during the DSS challenge and remained high after DSS was stopped. Clostridiaceae were more prominent in UC mice at baseline, but abundance fell in this group after DSS administration. In contrast, the abundance of Clostridiaceae increased at each time point in mice inoculated with stool from the healthy twin. *Lactobacillus* spp. were significantly more abundant in mice given healthy stool. The abundance of *Lactobacillus* spp. was less in UC mice. *Parasutterella* spp. were present only in mice inoculated with healthy stool, and their abundance increased slightly throughout the experiment, potentially due to inflammation.

**Metabolomics.** Stool samples collected from the mice after the DSS challenge on day 7 were analyzed in terms of metabolomics. With the exception of one outlier, the UC mice had a higher level of clustering (with R<sup>2</sup><sub>Y</sub>: 0.96 and Q<sup>2</sup>: 0.61) as compared with the other group, as shown in the orthogonal partial least squares-discriminant analysis (Orthogonal PLS-DA) (Figure 6). Seventeen metabolites differed significantly between the 2 groups of mice. However, only a small subset of these metabolites were annotated (that is, were clearly identifiable and found in the database we used). In the UC mice, the metabolites valyl-alanine, L-leucyl-L-alanine, valyl-valine, and 3-hydroxy-dodecane dioic acid were higher, and the metabolite 1-methylguanidine were lower (Table 4). Valyl-alanine, L-leucyl-L-alanine, and valyl-valine are dipeptides that result from incomplete protein digestion breakdown, whereas 1-methylguanidine is a modified purine. These findings suggest that mice inoculated with UC stool had more protein breakdown products and less cell damage than did mice that received the healthy stool.

**Table 2.** Mean relative abundances of bacteria significantly different between mice inoculated with stool from the UC-twin and the healthy cotwin, respectively, at the genus level. Mice inoculated with stool from the UC twin (UC) compared with mice inoculated with stool from the healthy twin (Healthy)

Bacteria	Human donors		Mice inoculated with stool from the UC-twin and the healthy cotwin, respectively, at the genus level											
	UC twin	Healthy twin	Day 1 (baseline)	UC	Healthy	Day 7 (after DSS)	UC	Healthy	Day 10 (euthanasia)	UC	Healthy	Cecum	UC	Healthy
Bacteroidaceae_Bacteroides*	15.96	0.00	↑<0.001	14.35	0.86	↑<0.001	20.37	3.54	↑<0.001	14.77	3.79	↑<0.001	8.15	2.30
Verrucomicrobiaceae_Akkermansia*	0.02	0.01	↑<0.001	4.43	0.02	↑<0.001	4.42	0.00	↑<0.001	5.11	0.00	↑<0.001	5.69	0.00
Enterobacteriaceae_Escherichia*	0.15	0.00	↑0.0103	2.98	0.00	↑0.0033	0.09	0.00	↑0.0131	0.10	0.00	↑0.0151	0.01	0.00
Clostridiaceae_Clostridium*	0.19	0.58	↑<0.001	1.54	0.44	↑<0.001	1.12	1.41	↑<0.001	1.19	1.97	↑<0.001	1.31	1.92
Lachnospiraceae_Coproccoccus*	0.52	0.24	↑ns	0.57	0.10	↑0.0012	0.25	0.34	↑0.0061	0.09	0.16	↑ns	0.28	0.30
Ruminococcaceae_Ruminococcus*	4.84	0.23	↑ns	0.54	0.46	↑0.0012	0.43	0.87	↑0.0061	1.32	0.42	↑0.001	0.70	0.18
Porphyromonadaceae_Parabacteroides	1.08	0.00	↑<0.001	0.53	0.00	↑<0.001	0.48	0.00	↑<0.001	0.57	0.01	↑<0.001	0.43	0.00
Rikenellaceae_Alistipes	1.44	0.25	↑<0.001	0.50	0.03	↑<0.001	0.08	0.03	↑<0.001	0.37	0.22	↑<0.001	0.19	0.63
Lachnospiraceae_Lachnospiraceae*	2.55	1.57	↑0.0023	0.07	0.12	↑0.0023	0.01	0.03	↓0.0367	0.00	0.05	↑<0.001	0.01	0.02
Prevotellaceae_Paraprevotella	1.37	0.00	↑<0.001	0.02	0.00	↑<0.001	2.11	0.00	↑<0.001	2.70	0.00	↑<0.001	1.28	0.00
Ruminococcaceae_Acetivibrio	0.00	0.00	↑0.0288	0.02	0.00	↑0.0288	0.00	0.06	↑<0.001	0.02	0.01	↑<0.001	0.02	0.02
Uncl. Enterobacteriaceae	0.00	0.00	↑0.0017	0.02	0.00	↑0.0017	0.00	0.00	↑<0.001	0.00	0.00	↑<0.001	0.00	0.00
Erysipelotrichaceae_Clostridium XVIII	0.00	0.00	↑ns	0.01	0.00	↑ns	0.00	0.00	↑ns	0.00	0.00	↑ns	0.00	0.00
Coriobacteriaceae_Enterorhabdus	0.00	0.00	↑ns	0.00	0.00	↑ns	0.00	0.01	↑0.0027	0.01	0.00	↑0.0022	0.01	0.01
Uncl. Bacteroidia	0.00	0.00	↓0.0021	8.50	21.23	↓0.0021	0.37	0.76	↑ns	3.03	1.53	↑ns	4.00	5.83
Lactobacillaceae_Lactobacillus*	0.00	0.08	↓<0.001	1.71	7.41	↓<0.001	0.49	1.45	↑ns	0.91	1.15	↑ns	1.83	1.09
Anaeroplasmataceae_Anaeroplasma	0.00	0.00	↓0.0036	1.35	2.24	↓0.0036	0.04	0.67	↑ns	0.17	0.52	↓0.002	0.06	0.43
Porphyromonadaceae_Odoribacter*	0.00	2.33	↓<0.001	0.00	1.16	↓<0.001	0.00	1.22	↓<0.001	0.00	1.42	↓<0.001	0.00	1.83
Sutterellaceae_Parasutterella	0.00	6.73	↓0.0017	0.00	0.43	↓0.0018	0.00	0.97	↓<0.001	0.00	1.31	↓<0.001	0.00	0.66
Ruminococcaceae_Pseudoflavonifractor*	0.00	0.05	↓<0.001	0.02	0.21	↓<0.001	0.07	0.26	↓<0.001	0.06	0.36	↓<0.001	0.06	0.58
Coriobacteriaceae_Adlercreutzia	0.00	0.03	↓0.0136	0.00	0.19	↓0.0136	0.00	0.00	↓<0.001	0.00	0.00	↓<0.001	0.00	0.00
Lachnospiraceae_Clostridium XIVb	0.11	0.01	↓ns	0.06	0.01	↓ns	0.02	0.06	↓0.0031	0.02	0.05	↓0.0031	0.03	0.08

Groups were compared by using the Kruskal-Wallis test followed by Conover-Iman test with Sidak correction for multiple comparisons. UC-inoc., mice inoculated with stool from the UC-twin; Healthy-inoc., mice inoculated with stool from the healthy cotwin; †, at termination; \*, genus contains short-chain fatty acid-producing bacteria; [†], (P value) and (Sidak-adjusted P value); †, decreased in UC-inoculated mice compared with healthy-inoculated mice; ‡, increased in UC-inoculated mice compared with healthy-inoculated mice; empty, no difference between groups; ns, not significant.



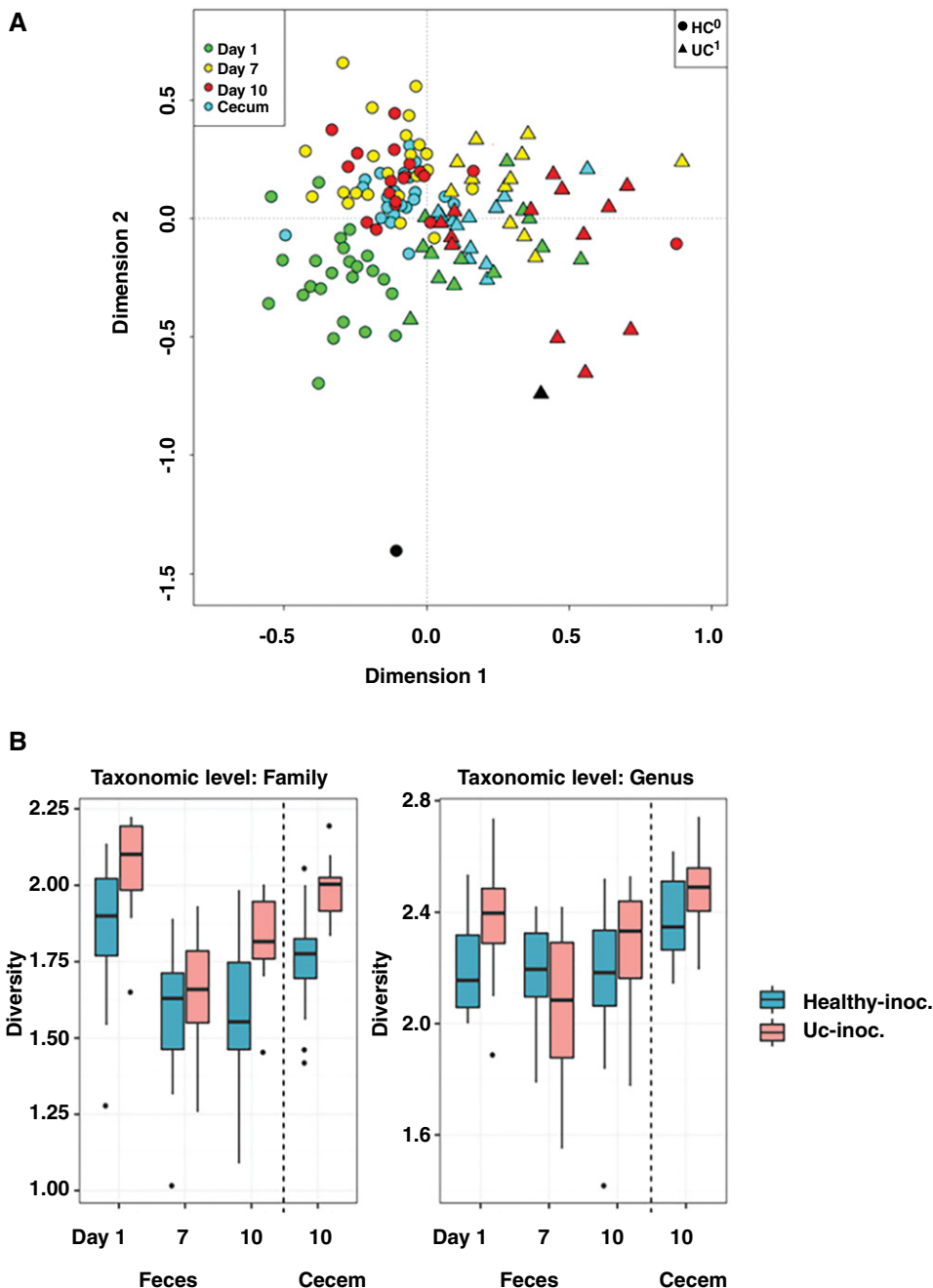


**Figure 5.** Bacterial composition of samples from human donors and inoculated mice. A nonmetric multidimensional scaling (nMDS) ordination plots from multivariate analysis. The input data were Bray-Curtis dissimilarity measures based on microbiota composition at family level. (A) nMDS score plots of stool samples and cecum content from mice inoculated with stool from the UC twin (UC) (colored triangles) and the healthy twin (Healthy) (colored circles). Colors represent different time points and sample types as follows: green: stool, day 1 ( $n$ : UC 13, Healthy 24); yellow: stool, day 7 ( $n$ : UC 12, Healthy 22); red: stool, day 10 ( $n$ : UC 13, Healthy 19); turquoise: cecum content, day 10 ( $n$ : UC 13, Healthy 21). Human donor stool samples from the UC twin (black triangle) and the healthy twin are also plotted (black circle). (B) Box plots of the bacterial diversity to illustrate the  $\alpha$  diversity (as measured by the Shannon index diversity) of stool samples from mice inoculated with stool from the healthy twin (blue) and the UC twin (red). This analysis was performed for 3 time points: day 1 (baseline), day 7 (after dextran sodium sulfate [DSS] challenge), and day 10 (at the end of the study, along with cecum content). The  $\alpha$  diversity was assessed at the taxonomic levels of family and genus. The results are presented graphically by using box plots that indicate the diversity changes over time and between the 2 groups of mice.

## Discussion

Our study documented distinct differences in the inflammatory potential of stool from 2 genetically identical human twins discordant for UC by transferring the stool to germ-free mice. Mice that received stool from the healthy twin had more severe histopathologic DSS-induced IBD than mice inoculated with stool from the healthy twin. This finding concurs with

a study of the gut microbiota composition of IBD-discordant monozygotic twin pairs that found that the gut microbiome of the healthy twin was more similar to that of IBD patients as compared with that of healthy individuals in terms of species composition and pathways related to butyrate biosynthesis.<sup>11</sup> Others have also recently used germ-free mice for transplantation of fecal matter from IBD patients and have shown that

**Table 3.** Mean relative abundances of bacteria significantly different between mice inoculated with stool from the UC-twin and the healthy cotwin, respectively, at the family level

Bacteria	Human donors		Mice inoculated with stool from the UC twin (UC-inoc.) compared with mice inoculated with stool from the healthy cotwin (Healthy-inoc.)												
	UC donor	Healthy donor	Day 1 (baseline)	Day 7 (after DSS)	UC-inoc.	Healthy-inoc.	Day 10 (+)	UC-inoc.	Healthy-inoc.	Cecum (+)	UC-inoc.	Healthy-inoc.			
Sutterellaceae	5.56	6.73	↓<0.001 ↓0.0025	↓<0.001 ↓<0.001	0.07	0.43	↓<0.001 ↓<0.001	0.00	0.97	↓<0.001 ↓<0.001	0.00	1.31	↓<0.001 ↓<0.001	0.00	0.66
Porphyromonadaceae*	4.39	2.35		↓0.0095 ↓ns	20.24	30.18		26.96	44.13		36.55	49.53	↓<0.001 ↓0.0129	24.25	35.29
Lactobacillaceae*	0.00	0.08	↓<0.001 ↓0.0017	↓0.0027 ↓ns	1.71	7.41		0.49	1.45		0.91	1.15		1.83	1.09
Coriobacteriaceae	1.57	1.40	↓<0.001 ↓0.0016		0.06	0.50		0.02	0.04		0.09	0.08		0.13	0.11
Uncl. Bacteroidia*	0.00	0.00	↓0.0041 ↓ns		9.98	21.23		0.80	1.19		3.72	4.32		4.19	7.21
Anaeroplasmataceae	0.00	0.00			1.35	2.24		0.04	0.67		0.17	0.52	↓0.002 ↓ns	0.06	0.43
Bacteroidaceae*	15.96	0.00	↑<0.001 ↑<0.001	↑<0.001 ↑<0.001	14.35	0.86		20.37	3.54	↑<0.001 ↑0.0034	14.77	3.79	↑<0.001 ↑0.0025	8.15	2.30
Verrucomicrobiaceae*	0.02	0.01	↑<0.001 ↑0.0048	↑<0.001 ↑0.0036	4.43	0.02		4.42	0.00	↑<0.001 ↑0.0074	5.11	0.00	↑<0.001 ↑0.0022	5.70	0.00
Prevotellaceae*	9.15	1.37		↑<0.001 ↑<0.001	0.02	0.00		2.11	0.00	↑<0.001 ↑<0.001	2.70	0.00	↑<0.001 ↑<0.001	1.28	0.00
Enterobacteriaceae*	0.15	0.02	↑<0.001 ↑<0.001	↑<0.001 ↑0.0017	3.00	0.01		0.09	0.01	↑<0.001 ↑0.023	0.10	0.01	↑<0.001 ↑<0.001	0.01	0.00
Rikenellaceae*	1.44	0.25	↑<0.001 ↑0.0011		0.50	0.03		0.08	0.03		0.37	0.22		0.19	0.63
Vallitalea	0.00	0.00	↑<0.001 ↑0.0134		0.30	0.09		0.22	0.10		0.09	0.11		0.39	0.16
Clostridiaceae*	0.23	0.65	↑0.0017 ↑0.0405		1.54	0.44		1.12	1.41		1.19	1.97		1.31	1.92

Comparisons were made with Kruskal-Wallis test followed by Conover-Iman test with Sidak correction for multiple comparisons. UC-inoc., mice inoculated with stool from the UC-twin; Healthy-inoc., mice inoculated with stool from the healthy cotwin; †, at termination; \*, family contains short-chain fatty acid-producing bacteria; [↓], (P value) and (Sidak-adjusted P value) ; ↓, decreased in UC-inoculated mice compared with healthy-inoculated mice; ↑, increased in UC-inoculated mice compared with healthy-inoculated mice; empty, no difference between groups; ns, not significant.

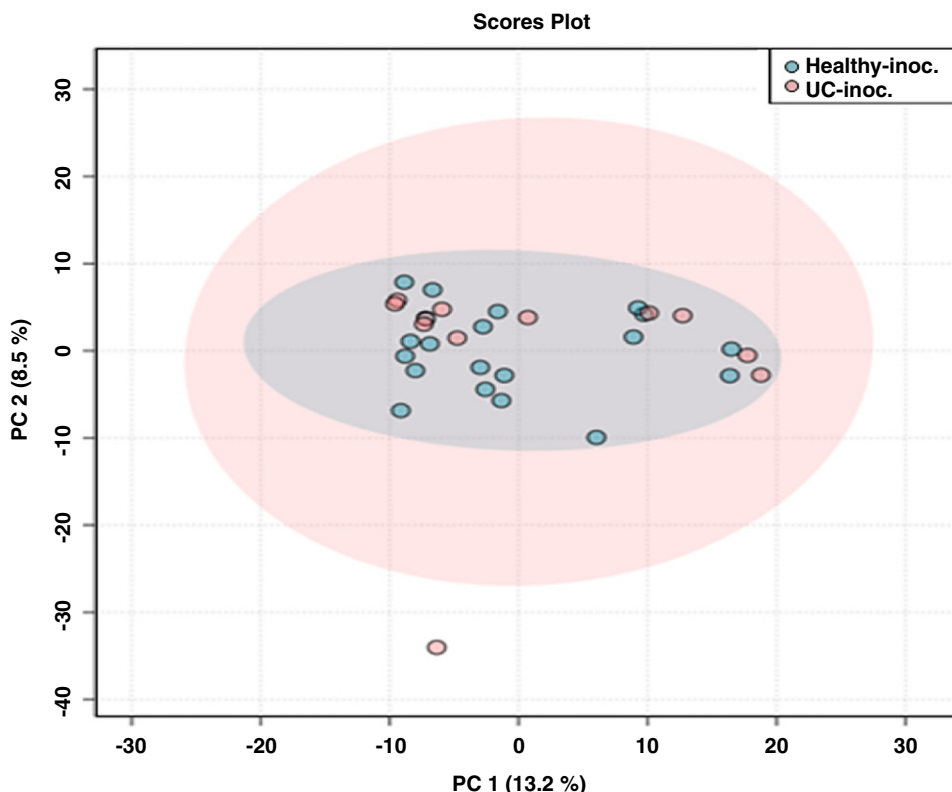


**Figure 6.** Visualization of the clustering of the metabolomic profiles of mice inoculated with stool from either the UC twin (UC, red;  $n = 12$ ) or the healthy twin (Healthy, blue,  $n = 20$ ) based on a principal component analysis (PCA) plot and depicting the relative distance scores of the principal component 1 (PC1 on the  $x$ -axis), which explains 13.2% of the differences in the metabolite composition, and the principal component 2 (PC2 on the  $y$ -axis), which explains 8.5% of the differences. The ellipses (clouds) are constructed to include the central 95% of the data based on the variance and covariance of the points of each group, and, therefore, can extend beyond the actual range of the data points observed. The larger cloud for the UC group suggests more variability in that group across the principal components analyzed. This analysis was conducted using high-performance liquid chromatography quadrupole time-of-flight mass spectrometry (HPLC-Q-TOF-MS).

specific traits of the human immune system, intestinal permeability, and clinical appearance are transferable<sup>69,72</sup> and that the phenotypic expression reflects the microbiome of the donor.<sup>5</sup> To our knowledge we are the first to use this tool to compare the phenotypes of mice transplanted with fecal matter from twins with discordant for IBD.

We found several significant distinctions in gut microbiota between our 2 groups of mice. Bacterial diversity, often regarded as indicative of a healthier microbiota,<sup>68</sup> was lower in mice inoculated with stool from the healthy twin. The abundance of both proinflammatory and antiinflammatory taxa was higher in mice that received stool from the UC twin. While the presence of mucin-degrading *Akkermansia* spp. was nearly absent in mice that received stool from the healthy twin, it was notably abundant in those mice inoculated with stool from the UC twin, despite the challenges normally associated with its transfer.<sup>25</sup> Enterobacteriaceae were more abundant in mice inoculated with stool from the UC twin (Table 3). Notably, the abundance of *Bacteroides* spp. was significantly higher in mice inoculated with stool from the UC twin, in contrast to its absence<sup>82</sup> and the prominent presence of *Dialister* spp.<sup>71</sup> in the healthy donor (Table 3). *Parabacteroides* spp. were predominantly found in UC-treated mice. This pattern may indicate a more inflammatory microbiota.

*Akkermansia* spp. is recognized for its antiinflammatory role,<sup>6</sup> and its abundance is typically diminished in IBD patients.<sup>58</sup> An increased abundance might be linked to a diet that is less disease-inducing.<sup>74</sup> In mice, *Akkermansia* spp. has potent anti-inflammatory effects,<sup>26</sup> exemplified by its ability to reduce the

**Table 4.** Metabolites that were significantly different in amount in feces of mice that received UC or healthy inocula

Metabolite	Class	UC compared with healthy
Valyl-alanine	Dipeptide	↑
L-leucyl-L-alanine	Dipeptide	↑
Valyl-valine	Dipeptide	↑
3-Hydroxydodecanedioic acid	Medium-chain hydroxy acid	↑
1-Methylguanine	6-Oxopurine	↓

incidence of type 1 diabetes.<sup>25,27</sup> Adjacent to the enterocytes, *Akkermansia* spp. generate the short-chain fatty acids (SCFAs) acetate and propionate.<sup>21</sup> Unlike bacteria such as *F. prausnitzii* that produce butyrate without mucin degradation capabilities, *Akkermansia* spp.'s mucin degradation facilitates close contact of butyrate with the enterocytes,<sup>53</sup> allowing SCFAs to signal to the host via the G protein-coupled receptors GPR41 and GPR43.<sup>13</sup> While some studies have linked Enterobacteriaceae with IBD,<sup>4</sup> early studies using mouse models showed that the LPS from enterobacteriaceal sources can induce a more tolerogenic state, thereby diminishing the susceptibility to both type 1 diabetes<sup>73</sup> and UC<sup>7</sup> later in life. Enterobacteriaceae also have a lower prevalence in UC patients as compared with the general population.<sup>1</sup> Healthy humans may not harbor *Bacteroides* spp., although its presence is more common.<sup>70</sup> Healthy humans normally show greater diversity early in life.<sup>70</sup> In one study, the depletion of *Bacteroides* spp. was correlated with IBD in human

patients.<sup>82</sup> In another study, a subset of the clinically active UC patients had an overabundance of proteases that originated from *Bacteroides vulgatus*, and use of a broad-spectrum protease inhibitor prevented colitis from developing in *B. vulgatus* mono-colonized, IL-10 deficient mice.<sup>46</sup> Furthermore, transplantation of feces from UC patients with a high abundance of *B. vulgatus* proteases into germ-free mice induced protease-dependent colitis. Although *Bacteroides* spp. also contain LPS in their cell walls, their capacity to induce an antiinflammatory response in children is potentially less than that of enterobacteriaceal LPS and therefore they, also give children less protection against development of inflammatory diseases later in life.<sup>73</sup> *Parabacteroides* spp. are reportedly diminished in IBD cases as compared with healthy controls.<sup>83</sup> Oral administration of a specific antigen derived from *Parabacteroides distasonis* can alleviate DSS-induced colitis by activating innate and adaptive immunomodulatory mechanisms.<sup>34</sup>

Our metabolomics analysis corroborated the concept of antiinflammatory gut microbiota in mice that received stool from the UC twin. Substances like valyl-alanine and 3-hydroxydodecanoic acid, which have previously exhibited antiinflammatory properties in mice subjected to 5-aminosalicylic acid treatment,<sup>45,48</sup> were detected. Previous research has associated drug interventions and resultant lower disease activity with alterations in the gut microbiota of both UC and rheumatoid arthritis patients.<sup>20,50</sup> Consequently, prior and ongoing clinical treatment of the UC twin may have mitigated the inflammatory potential of her gut microbiota. Conversely, the gut microbiota of the untreated healthy twin had a more inflammatory profile. Finally, differences in the dietary habits of these twins could also have influenced their microbiota composition and metabolism.<sup>15,31</sup>

Mouse studies provide fundamental insights for research; however, translating findings from mice to humans is not always feasible due to the dissimilarities between species. Moreover, not all human taxa can be effectively transferred to mice,<sup>41</sup> and the low colonization efficiency we observed is comparable with similar studies.<sup>41,78</sup> The antiinflammatory bacterium *F. prausnitzii*, a potential catalyst for the favorable effects of a less disease-inducing diet in human patients,<sup>74</sup> was naturally abundant in our donor inocula, consistent with its abundance in humans.<sup>38</sup> However, as in other human microbiota transfer studies,<sup>41</sup> *F. prausnitzii* did not become well established in our inoculated mice. Such failed transfers might significantly affect the disease phenotype of the mice. Also, we did not consider the transfer of viral communities, which can have an effect on the obese phenotype in mice.<sup>59</sup> A limitation of germ-free mouse studies is that using a large number of donors is impossible for studies in which all groups need a dedicated isolator; consequently, our findings could be specific to specific individuals and not applicable to all human donors. Furthermore, the mouse immune response to the human microbiota is known to be inadequate with respect to the generation of T cells,<sup>19</sup> further complicating the transfer of human microbiota to germ-free mice. Future studies should include an uninoculated group of mice and a group inoculated with stool from recently diagnosed and untreated IBD patients. This comprehensive approach would provide a more holistic understanding of the dynamics at play.

The goal of our study was to assess the colitis-inducing potential of microbiota transplantation from a UC-discordant twin pair. In our study, mice that received stool from the healthy twin had significantly greater colon inflammation upon DSS induction. This observation suggests that germ-free mice can be used as a tool to show that the healthy twin had a gut microbiota with

greater inflammatory tendencies than that of the UC-diagnosed twin. This conclusion is bolstered by the disparities observed in the 2 twins with regard to their gut microbiota composition.

## Acknowledgments

We thank Sofie Kromann for creating the histological photographs and Helene Farlov and Mette Nelander for taking care of the mice.

## Conflict of Interest

The author(s) have no conflict(s) to disclose.

## Funding

The Lundbeck Foundation (grant numbers R208-2015-3060, R211-2015-3061), Region of Southern Denmark, University Hospital of Southern Denmark, Knud og Edith Eriksens Mindefond, and The A.P. Møller Foundation for the Advancement of Medical Science. IBD-CARE (V Andersen).

## References

1. Alam MT, Amos GCA, Murphy ARJ, Murch S, Wellington EMH, Arasaradnam RP. 2020. Microbial imbalance in inflammatory bowel disease patients at different taxonomic levels. *Gut Pathog* 12:1. <https://doi.org/10.1186/s13099-019-0341-6>.
2. Ananthakrishnan AN. 2015. Epidemiology and risk factors for IBD. *Nat Rev Gastroenterol Hepatol* 12:205–217. <https://doi.org/10.1038/nrgastro.2015.34>.
3. Andersen V, Hansen AK, Heitmann BL. 2017. Potential impact of diet on treatment effect from anti-tnf drugs in inflammatory bowel disease. *Nutrients* 9:326. <https://doi.org/10.3390/nu9030286>.
4. Baldelli V, Scaldaferrri F, Putignani L, Del Chierico F. 2021. The role of Enterobacteriaceae in gut microbiota dysbiosis in inflammatory bowel diseases. *Microorganisms* 9:697. <https://doi.org/10.3390/microorganisms9040697>.
5. Basson AR, Gomez-Nguyen A, Menghini P, Buttó LF, Di Martino L, Aladyshkina N, Osme A, et al. 2020. Human gut microbiome transplantation in ileitis prone mice: A tool for the functional characterization of the microbiota in inflammatory bowel disease patients. *Inflamm Bowel Dis* 26:347–359.
6. Belzer C, de Vos WM. 2012. Microbes inside—From diversity to function: The case of Akkermansia. *ISME J* 6:1449–1458. <https://doi.org/10.1038/ismej.2012.6>.
7. Bendtsen KM, Hansen CHE, Krych L, Skovgaard K, Kot W, Vogensen FK, Hansen AK. 2017. Immunological effects of reduced mucosal integrity in the early life of BALB/c mice. *PLoS One* 12:e0176662. <https://doi.org/10.1371/journal.pone.0176662>.
8. Bendtsen KM, Tougaard P, Hansen AK. 2018. An early life mucosal insult temporarily decreases acute oxazolone-induced inflammation in mice. *Inflammation* 41:1437–1447. <https://doi.org/10.1007/s10753-018-0790-y>.
9. Betsou F, Lehmann S, Ashton G, Barnes M, Benson EE, Coppola D, DeSouza Y, et al. 2010. Standard preanalytical coding for biospecimens: Defining the sample PREanalytical code. *Cancer Epidemiol Biomarkers Prev* 19:1004–1011. <https://doi.org/10.1158/1055-9965.EPI-09-1268>.
10. Bleich A, Mähler M, Most C, Leiter EH, Liebler-Tenorio E, Elson CO, Hedrich HJ, Schlegelberger B, Sundberg JP. 2004. Refined histopathologic scoring system improves power to detect colitis QTL in mice. *Mamm Genome* 15:865–871. <https://doi.org/10.1007/s00335-004-2392-2>.
11. Brand EC, Klaassen MAY, Gacesa R, Vich Vila A, Ghosh H, de Zoete MR, Boomsma DI, et al. 2021. Healthy cotwins share gut microbiome signatures with their inflammatory bowel disease twins and unrelated patients. *Gastroenterology* 160:1970–1985. <https://doi.org/10.1053/j.gastro.2021.01.030>.
12. Britton GJ, Contijoch EJ, Mogno I, Vennaro OH, Llewellyn SR, Ng R, Li Z, et al. 2019. Microbiotas from humans with inflammatory bowel disease alter the balance of gut Th17 and RORgammat(+) regulatory T cells and exacerbate colitis in mice. *Immunity* 50:212–224.e214. <https://doi.org/10.1016/j.immuni.2018.12.015>.

13. **Brown AJ, Goldsworthy SM, Barnes AA, Eilert MM, Tcheang L, Daniels D, Muir AI, et al.** 2003. The Orphan G protein-coupled receptors GPR41 and GPR43 are activated by propionate and other short chain carboxylic acids. *J Biol Chem* **278**:11312–11319. <https://doi.org/10.1074/jbc.M211609200>.
14. **Caccaro R, Angriman I, D'Incà R.** 2016. Relevance of fecal calprotectin and lactoferrin in the post-operative management of inflammatory bowel diseases. *World J Gastrointest Surg* **8**:193–201. <https://doi.org/10.4240/wjgs.v8.i3.193>.
15. **Campmans-Kuijpers MJE, Dijkstra G.** 2021. Food and food groups in inflammatory bowel disease (IBD): The design of the groningen anti-inflammatory diet (GrAID). *Nutrients* **13**:1067. <https://doi.org/10.3390/nu13041067>.
16. **Centers for Disease Control and Prevention.** [Internet]. 2021. Defining adult overweight & obesity. [Cited 9 March 2024]. Available at: <https://www.cdc.gov/obesity/adult/basics/defining.html>.
17. **Chang JT.** 2020. Pathophysiology of inflammatory bowel diseases. *N Engl J Med* **383**:2652–2664. <https://doi.org/10.1056/NEJMra2002697>.
18. **Chong J, Soufan O, Li C, Caraus I, Li S, Bourque G, Wishart DS, Xia J.** 2018. MetaboAnalyst 4.0: Towards more transparent and integrative metabolomics analysis. *Nucleic Acids Res* **46** W1:W486–W494. <https://doi.org/10.1093/nar/gky310>.
19. **Chung H, Pamp SJ, Hill JA, Surana NK, Edelman SM, Troy EB, Reading NC, et al.** 2012. Gut immune maturation depends on colonization with a host-specific microbiota. *Cell* **149**:1578–1593. <https://doi.org/10.1016/j.cell.2012.04.037>.
20. **Crouwel F, Buijter HJC, de Boer NK.** 2021. Gut microbiota-driven drug metabolism in inflammatory bowel disease. *J Crohn's Colitis* **15**:307–315. <https://doi.org/10.1093/ecco-jcc/jjaa143>.
21. **Derrien M, Van Baarlen P, Hooiveld G, Norin E, Muller M, de Vos WM.** 2011. Modulation of mucosal immune response, tolerance, and proliferation in mice colonized by the mucin-degrader *Akkermansia muciniphila*. *Front Microbiol* **2**:166. <https://doi.org/10.3389/fmicb.2011.00166>.
22. **GBD 2017 Inflammatory Bowel Disease Collaborators.** 2020. The global, regional, and national burden of inflammatory bowel disease in 195 countries and territories, 1990–2017: A systematic analysis for the Global Burden of Disease Study 2017. *Lancet Gastroenterol Hepatol* **5**:17–30. [https://doi.org/10.1016/S2468-1253\(19\)30333-4](https://doi.org/10.1016/S2468-1253(19)30333-4).
23. **Goodman AL, Kallstrom G, Faith JJ, Reyes A, Moore A, Dantas G, Gordon JL.** 2011. Extensive personal human gut microbiota culture collections characterized and manipulated in gnotobiotic mice. *Proc Natl Acad Sci USA* **108**:6252–6257. <https://doi.org/10.1073/pnas.1102938108>.
24. **Gordon H, Trier Moller F, Andersen V, Harbord M.** 2015. Heritability in inflammatory bowel disease: From the first twin study to genome-wide association studies. *Inflamm Bowel Dis* **21**:1428–1434. <https://doi.org/10.1097/MIB.0000000000000393>.
25. **Hanninen A, Toivonen R, Poysti S, Belzer C, Plovier H, Ouverkerk JP, Emani R, et al.** 2018. *Akkermansia muciniphila* induces gut microbiota remodelling and controls islet autoimmunity in NOD mice. *Gut* **67**:1445–1453. <https://doi.org/10.1136/gutjnl-2017-314508>.
26. **Hansen AK, Nielsen DS, Krych L, Hansen CHF.** 2019. Bacterial species to be considered in quality assurance of mice and rats. *Lab Anim* **53**:281–291. <https://doi.org/10.1177/0023677219834324>.
27. **Hansen CH, Krych L, Nielsen DS, Vogensen FK, Hansen LH, Sorensen SJ, Buschard K, et al.** 2012. Early life treatment with vancomycin propagates *Akkermansia muciniphila* and reduces diabetes incidence in the NOD mouse. *Diabetologia* **55**:2285–2294. <https://doi.org/10.1007/s00125-012-2564-7>.
28. **Havelund JE, Andersen AD, Binzer M, Blaabjerg M, Heegaard NHH, Stenager E, Faergeman NJ, et al.** 2017. Changes in kynurenine pathway metabolism in Parkinson patients with L-DOPA-induced dyskinesia. *J Neurochem* **142**:756–766. <https://doi.org/10.1111/jnc.14104>.
29. **Holgerson K, Kvist PH, Hansen AK, Holm TL.** 2014. Predictive validity and immune cell involvement in the pathogenesis of piroxicam-accelerated colitis in interleukin-10 knockout mice. *Int Immunopharmacol* **21**:137–147. <https://doi.org/10.1016/j.intimp.2014.04.017>.
30. **Huang EY, Inoue T, Leone VA, Dalal S, Touw K, Wang Y, Musch MW, et al.** 2015. Using corticosteroids to reshape the gut microbiome: Implications for inflammatory bowel diseases. *Inflamm Bowel Dis* **21**:963–972. <https://doi.org/10.1097/MIB.0000000000000332>.
31. **Jiang Y, Jarr K, Layton C, Gardner CD, Ashouri JF, Abreu MT, Sinha SR.** 2021. Therapeutic implications of diet in inflammatory bowel disease and related immune-mediated inflammatory diseases. *Nutrients* **13**:890. <https://doi.org/10.3390/nu13030890>.
32. **Khang X, Jia M, Zhao L, Zhang S.** [Internet]. 2021. 2.2.1. Disease activity index (DAI). [Cited 9 March 2024]. Available at: <https://bio-protocol.org/exchange/minidetail?type=30&id=9164061>.
33. **Kobayashi T, Siegmund B, Le Berre C, Wei SC, Ferrante M, Shen B, Bernstein CN, Danese S, Peyrin-Biroulet L, Hibi T.** 2020. Ulcerative colitis. *Nat Rev Dis Primers* **6**:74. <https://doi.org/10.1038/s41572-020-0205-x>.
34. **Kverka M, Zakostelska Z, Klimesova K, Sokol D, Hudcovic T, Hrcir T, Rossmann P, et al.** 2011. Oral administration of *Parabacteroides distasonis* antigens attenuates experimental murine colitis through modulation of immunity and microbiota composition. *Clin Exp Immunol* **163**:250–259. <https://doi.org/10.1111/j.1365-2249.2010.04286.x>.
35. **Lees CW, Barrett JC, Parkes M, Satsangi J.** 2011. New IBD genetics: Common pathways with other diseases. *Gut* **60**:1739–1753. <https://doi.org/10.1136/gut.2009.199679>.
36. **Lim MY, You HJ, Yoon HS, Kwon B, Lee JY, Lee S, Song YM, Lee K, Sung J, Ko G.** 2017. The effect of heritability and host genetics on the gut microbiota and metabolic syndrome. *Gut* **66**:1031–1038. <https://doi.org/10.1136/gutjnl-2015-311326>.
37. **Liu F, Ma R, Riordan SM, Grimm MC, Liu L, Wang Y, Zhang L.** 2017. Azathioprine, mercaptopurine, and 5-aminosalicylic acid affect the growth of IBD-associated *Campylobacter* species and other enteric microbes. *Front Microbiol* **8**:527. <https://doi.org/10.3389/fmicb.2017.00527>.
38. **Lopez-Siles M, Duncan SH, Garcia-Gil LJ, Martinez-Medina M.** 2017. *Faecalibacterium prausnitzii*: from microbiology to diagnostics and prognostics. *ISME J* **11**:841–852. <https://doi.org/10.1038/ismej.2016.176>.
39. **Lu K, Abo RP, Schlieper KA, Graffam ME, Levine S, Wishnok JS, Swenberg JA, Tannenbaum SR, Fox JG.** 2014. Arsenic exposure perturbs the gut microbiome and its metabolic profile in mice: An integrated metagenomics and metabolomics analysis. *Environ Health Perspect* **122**:284–291. <https://doi.org/10.1289/ehp.1307429>.
40. **Lundberg R, Bahl MI, Licht TR, Toft MF, Hansen AK.** 2017. Microbiota composition of simultaneously colonized mice housed under either a gnotobiotic isolator or individually ventilated cage regime. *Sci Rep* **7**:42245. <https://doi.org/10.1038/srep42245>.
41. **Lundberg R, Toft MF, Metzdorff SB, Hansen CHF, Licht TR, Bahl MI, Hansen AK.** 2020. Human microbiota-transplanted C57BL/6 mice and offspring display reduced establishment of key bacteria and reduced immune stimulation compared to mouse microbiota-transplantation. *Sci Rep* **10**:7805. <https://doi.org/10.1038/s41598-020-64703-z>.
42. **Magnusson MK, Strid H, Sapnara M, Lasso A, Bajor A, Ung KA, Ohman L.** 2016. Anti-TNF therapy response in patients with ulcerative colitis is associated with colonic antimicrobial peptide expression and microbiota composition. *J Crohns Colitis* **10**:943–952. <https://doi.org/10.1093/ecco-jcc/jjw051>.
43. **Mahler Convenor M, Berard M, Feinstein R, Gallagher A, Illgen-Wilcke B, Pritchett-Corning K, Raspa M.** 2014. FELASA recommendations for the health monitoring of mouse, rat, hamster, guinea pig and rabbit colonies in breeding and experimental units. *Lab Anim* **48**:178–192. <https://doi.org/10.1177/0023677213516312>.
44. **Mentella MC, Scaldaferrri F, Pizzoferrato M, Gasbarrini A, Migliano GAD.** 2020. Nutrition, IBD and gut microbiota: A review. *Nutrients* **12**:12. <https://doi.org/10.3390/nu12040944>.

45. Meyers BE, Moonka DK, Davis RH. 1979. The effect of selected amino acids on gelatin-induced inflammation in adult male mice. *Inflammation* 3:225–233. <https://doi.org/10.1007/BF00914179>.
46. Mills RH, Dulai PS, Vázquez-Baeza Y, Saucedo C, Daniel N, Gerner RR, Batachari LE, et al. 2022. Multi-omics analyses of the ulcerative colitis gut microbiome link *Bacteroides vulgatus* proteases with disease severity. *Nat Microbiol* 7:262–276. <https://doi.org/10.1038/s41564-021-01050-3>.
47. Møller FT, Knudsen L, Harbord M, Satsangi J, Gordon H, Christiansen L, Christensen K, Jess T, Andersen V. 2016. Danish cohort of monozygotic inflammatory bowel disease twins: Clinical characteristics and inflammatory activity. *W J Gastroenterol* 22:5050–5059. <https://doi.org/10.3748/wjg.v22.i21.5050>.
48. Molteni M, Bosi A, Rossetti C. 2018. Natural products with Toll-like receptor 4 antagonist activity. *Int J Inflamm* 2018:2859135. <https://doi.org/10.1155/2018/2859135>.
49. Moore HM, Kelly A, Jewell SD, McShane LM, Clark DP, Greenspan R, Hainaut P, et al. 2011. Biospecimen reporting for improved study quality. *Biopreserv Biobank* 9:57–70. <https://doi.org/10.1089/bio.2010.0036>.
50. Nayak RR, Alexander N, Deshpande I, Stapleton-Gray K, Rimal B, Patterson AD, Ubeda C, et al. 2021. Methotrexate impacts conserved pathways in diverse human gut bacteria leading to decreased host immune activation. *Cell Host Microbe* 29:362–377. e311. <https://doi.org/10.1016/j.chom.2020.12.008>.
51. Nishida A, Inoue R, Inatomi O, Bamba S, Naito Y, Andoh A. 2018. Gut microbiota in the pathogenesis of inflammatory bowel disease. *Clin J Gastroenterol* 11:1–10. <https://doi.org/10.1007/s12328-017-0813-5>.
52. Oksanen J, Blanchet FG, Friendly M, Kindt R, Legendre P, McGinn D, Minchin PR, et al. [Internet]. *Vegan: Community ecology package*. R package version 2.5-4. [Cited 9 March 2024]. Available at: <https://CRAN.R-project.org/package=vegan>.
53. Ottman N, Geerlings SY, Aalvink S, de Vos WM, Belzer C. 2017. Action and function of *Akkermansia muciniphila* in microbiome ecology, health and disease. *Best Pract Res Clin Gastroenterol* 31:637–642. <https://doi.org/10.1016/j.bpg.2017.10.001>.
54. Pathirana WGW, Chubb SP, Gillett MJ, Vasikaran SD. 2018. Faecal calprotectin. *Clin Biochem Rev* 39:77–90.
55. Order on the Animal Experimentation Act. [Internet]. 2017. LBK 1107 of July 1, 2022. [Cited 9 March 2024]. Available at: <https://www.retsinformation.dk/eli/lta/2022/1107>.
56. Percie du Sert N, Hurst V, Ahluwalia A, Alam S, Avey MT, Baker M, Browne WJ, et al. 2020. The ARRIVE guidelines 2.0: Updated guidelines for reporting animal research. *PLoS Biol* 18:e3000410. <https://doi.org/10.1371/journal.pbio.3000410>.
57. Pluskal T, Castillo S, Villar-Briones A, Oresic M. 2010. MZmine 2: Modular framework for processing, visualizing, and analyzing mass spectrometry-based molecular profile data. *BMC Bioinformatics* 11:395. <https://doi.org/10.1186/1471-2105-11-395>.
58. Png CW, Linden SK, Gilshenan KS, Zoetendal EG, McSweeney CS, Sly LI, McGuckin MA, et al. 2010. Mucolytic bacteria with increased prevalence in IBD mucosa augment in vitro utilization of mucin by other bacteria. *Am J Gastroenterol* 105:2420–2428. <https://doi.org/10.1038/ajg.2010.281>.
59. Rasmussen TS, Mentzel CMJ, Kot W, Castro-Mejia JL, Zuffa S, Swann JR, Hansen LH, et al. 2020. Faecal virome transplantation decreases symptoms of type 2 diabetes and obesity in a murine model. *Gut* 69:2122–2130. <https://doi.org/10.1136/gutjnl-2019-320005>.
60. Ridaura VK, Faith JJ, Rey FE, Cheng J, Duncan AE, Kau AL, Griffin NW, et al. 2013. Gut microbiota from twins discordant for obesity modulate metabolism in mice. *Science* 341:1241214. <https://doi.org/10.1126/science.1241214>.
61. Round JL, Mazmanian SK. 2010. Inducible Foxp3+ regulatory T-cell development by a commensal bacterium of the intestinal microbiota. *Proc Natl Acad Sci USA* 107:12204–12209. <https://doi.org/10.1073/pnas.0909122107>.
62. Salek RM, Steinbeck C, Viant MR, Goodacre R, Dunn WB. 2013. The role of reporting standards for metabolite annotation and identification in metabolomic studies. *Gigascience* 2:13. <https://doi.org/10.1186/2047-217X-2-13>.
63. Sartor RB. 2008. Microbial influences in inflammatory bowel diseases. *Gastroenterology* 134:577–594. <https://doi.org/10.1053/j.gastro.2007.11.059>.
64. Sartor RB, Wu GD. 2017. Roles for intestinal bacteria, viruses, and fungi in pathogenesis of inflammatory bowel diseases and therapeutic approaches. *Gastroenterology* 152:327–339. <https://doi.org/10.1053/j.gastro.2016.10.012>.
65. Sheehan D, Moran C, Shanahan F. 2015. The microbiota in inflammatory bowel disease. *J Gastroenterol* 50:495–507. <https://doi.org/10.1007/s00535-015-1064-1>.
66. Smith AJ, Clutton RE, Lilley E, Hansen KEA, Brattelid T. 2018. PREPARE: Guidelines for planning animal research and testing. *Lab Anim* 52:135–141. <https://doi.org/10.1177/0023677217724823>.
67. Sokol H, Pigneur B, Watterlot L, Lakhdari O, Bermudez-Humaran LG, Gratadoux JJ, Blugeon S, et al. 2008. *Faecalibacterium prausnitzii* is an anti-inflammatory commensal bacterium identified by gut microbiota analysis of Crohn disease patients. *Proc Natl Acad Sci USA* 105:16731–16736. <https://doi.org/10.1073/pnas.0804812105>.
68. Sommer F, Anderson JM, Bharti R, Raes J, Rosenstiel P. 2017. The resilience of the intestinal microbiota influences health and disease. *Nat Rev Microbiol* 15:630–638. <https://doi.org/10.1038/nrmicro.2017.58>.
69. Souza ÉL, Elian SD, Paula LM, Garcia CC, Vieira AT, Teixeira MM, Arantes RM, Nicoli JR, Martins FS. 2016. *Escherichia coli* strain Nissle 1917 ameliorates experimental colitis by modulating intestinal permeability, the inflammatory response and clinical signs in a faecal transplantation model. *J Med Microbiol* 65:201–210. <https://doi.org/10.1099/jmm.0.000222>.
70. Stewart CJ, Ajami NJ, O'Brien JL, Hutchinson DS, Smith DP, Wong MC, Ross MC, et al. 2018. Temporal development of the gut microbiome in early childhood from the TEDDY study. *Nature* 562:583–588. <https://doi.org/10.1038/s41586-018-0617-x>.
71. Tito RY, Cypers H, Joossens M, Varkas G, Van Praet L, Glorieux E, Van den Bosch F, De Vos M, Raes J, Elewaut D. 2017. Brief report: Dialister as a microbial marker of disease activity in spondyloarthritis. *Arthritis Rheumatol* 69:114–121. <https://doi.org/10.1002/art.39802>.
72. Torres J, Hu J, Seki A, Eisele C, Nair N, Huang R, Tarassishin L, et al. 2020. Infants born to mothers with IBD present with altered gut microbiome that transfers abnormalities of the adaptive immune system to germ-free mice. *Gut* 69:42–51. <https://doi.org/10.1136/gutjnl-2018-317855>.
73. Vatanen T, Kostic AD, d'Hennezel E, Siljander H, Franzosa EA, Yassour M, Kolde R, et al. 2016. Variation in microbiome LPS immunogenicity contributes to autoimmunity in humans. *Cell* 165:842–853. <https://doi.org/10.1016/j.cell.2016.04.007>.
74. Verhoog S, Taneri PE, Roa Diaz ZM, Marques-Vidal P, Troup JP, Bally L, Franco OH, Glisic M, Muka T. 2019. Dietary factors and modulation of bacteria strains of *Akkermansia muciniphila* and *Faecalibacterium prausnitzii*: A systematic review. *Nutrients* 11:1565. <https://doi.org/10.3390/nu11071565>.
75. Vester-Andersen MK, Mirsepasi-Lauridsen HC, Prosborg MV, Mortensen CO, Trager C, Skovsen K, Thorkilgaard T, et al. 2019. Increased abundance of proteobacteria in aggressive Crohn's disease seven years after diagnosis. *Sci Rep* 9:13473. <https://doi.org/10.1038/s41598-019-49833-3>.
76. Walker AW, Sanderson JD, Churcher C, Parkes GC, Hudspith BN, Rayment N, Brostoff J, Parkhill J, Dougan G, Petrovska L. 2011. High-throughput clone library analysis of the mucosa-associated microbiota reveals dysbiosis and differences between inflamed and non-inflamed regions of the intestine in inflammatory bowel disease. *BMC Microbiol* 11:7. <https://doi.org/10.1186/1471-2180-11-7>.
77. Walmsley RS, Ayres RC, Pounder RE, Allan RN. 1998. A simple clinical colitis activity index. *Gut* 43:29–32. <https://doi.org/10.1136/gut.43.1.29>.
78. Wos-Oxley M, Bleich A, Oxley AP, Kahl S, Janus LM, Smoczek A, Nahrstedt H, et al. 2012. Comparative evaluation of establishing a human gut microbial community within rodent models. *Gut Microbes* 3:234–249. <https://doi.org/10.4161/gmic.19934>.
79. Wu GD, Lewis JD, Hoffmann C, Chen YY, Knight R, Bittinger K, Hwang J, et al. 2010. Sampling and pyrosequencing methods for characterizing bacterial communities in the human gut using 16S sequence tags. *BMC Microbiol* 10:206. <https://doi.org/10.1186/1471-2180-10-206>.

80. **Xu J, Chen N, Wu Z, Song Y, Zhang Y, Wu N, Zhang F, Ren X, Liu Y.** 2018. 5-Aminosalicylic acid alters the gut bacterial microbiota in patients with ulcerative colitis. *Front Microbiol* **9**:1274. <https://doi.org/10.3389/fmicb.2018.01274>.
81. **Zachariassen LF, Hansen AK, Krych L, Nielsen DS, Holm TL, Tougaard P, Hansen CHF.** 2019. Cesarean section increases sensitivity to oxazolone-induced colitis in C57BL/6 mice. *Mucosal Immunol* **12**:1348–1357. <https://doi.org/10.1038/s41385-019-0207-8>.
82. **Zhou Y, Zhi F.** 2016. Lower level of bacteroides in the gut microbiota is associated with inflammatory bowel disease: A meta-analysis. *BioMed Res Int* **2016**:5828959. <https://doi.org/10.1155/2016/5828959>.
83. **Zitomersky NL, Atkinson BJ, Franklin SW, Mitchell PD, Snapper SB, Comstock LE, Bousvaros A.** 2013. Characterization of adherent bacteroidales from intestinal biopsies of children and young adults with inflammatory bowel disease. *PLoS One* **8**:e63686. <https://doi.org/10.1371/journal.pone.0063686>.